International Journal of Aviation Science and Engineering
e-ISSN: 2715-6958 p-ISSN: 2721-5342

AVIA

Original Article

Conceptual Design of a 10-Seater Electric Aircraft

A Marcell, F Limor, J F Humairah, M D T Z Baniz, and Taufiq Mulyanto *

Faculty of Aerospace Engineering, Institute Technology of Bandung, Kota Bandung, Jawa Barat 40132 Indonesia

* Correspondence: taufiq.mulyanto@ae.itb.ac.id

Received: 13 August 2023; Accepted: 8 October 2023; Published: 1 December 2023

With the increase in population, an increase of transportation needs is inevitable, especially in air travel. There is an underlying problem in this matter that is carbon pollutions. Air travel contributes around 2% of the global emissions. This paper contains the conceptual design of 10- seater electric aircraft that can serve as a cleaner alternative for air travel. The paper will discuss about our objectives and the results of configurations, backed with calculations of proof in all aspects that is needed. In conclusions, this paper presents a conceptual design of 10-seater electric aircraft that have range more than 450 km. The aircraft being designed has a mid-wing three surface configuration with a MTOW of 7250 kg

Keywords: electric aircraft; 10-seater aircraft; conceptual design

1. Introduction

Environmental problems are a big issue in this modern world. The airline industry contributes to 2.5% of the global carbon emissions, and that number is increasing, exponentially. While there are some airlines that started offsetting their contributions to atmospheric carbon, significant cutbacks are still needed.

Electric aircraft provides a better solution to eliminate direct carbon emission, reduce the cost of fuel, maintenance, and also noise. Electric aircraft also proves to be more cost efficient in the operation aspect, needing to overhaul the motors at 20,000 hours instead of 2,000. However, as of today, electric aircraft are still limited with the current technology. Creating a battery as compact as fuel will need another development for years to come. Even then, potential engineers need to take the step, showing the world that electric aircraft exist and are comparable to the conventional ones in some mission cases. With that in mind, this paper shows the design processes in designing an electric aircraft with specific requirements.

Design requirement and objective (DRO) is given to guide the design of the aircraft. This guidance is going to help produce an electric aircraft that fulfills the design requirement and objectives as efficiently as possible while maintaining a high standard in looks, regulations, cost, and manufacturability. The DRO is shown in Table 1 as follows.

2. Materials and Methods

Design process started with the study of several reference aircrafts which are considered have a certain characteristic that are useful for the designed aircraft. There are four aircrafts taken as reference, two are electric aircrafts which have 10 to 11 seats and the other two are turbo prop and piston engine aircraft which have interesting configuration. Table 2 presents data of reference aircrafts. This referenced aircraft is considered to be the closest as possible in terms of missions and configurations.

e-ISSN: 2715-6958 p-ISSN: 2721-5342

Table 1. Design Requirement Objective

General		Cabin and Instruments		
Capacity	10 seats	Flight Crew	1-2 crew	
MTOW	8000 kg | 17637 lbs	Passengers	8-9 pax	
Propulsion	Electric	Cabin Volume	≥ 9 m3	
Battery	>260 Wh/kg	Baggage Volume	≥ 1.6 m3	
Certified Year	2026	Weight / Pax	Passengers	90 kg
Price	< $3.6 million		Baggage	10 kg

Performance			
Payload	**Range**	**Velocity**	**Altitude**
Max Payload	≥ 450 km	≥ 250 km/h	10000 ft
4 Passengers	≥ 550 km	≥ 259 km/h	10000 ft

Performance		
Take Off distance (Sea Level ISA +15)	MTOW	≤ 900 m
Landing distance (Sea Level ISA +15)	0.95 MTOW	≤ 950 m
Rate of Climb (Sea Level)	MTOW	≥ 1600 fpm

Table 2. Referenced Aircraft

	Eviation Alice	**eFlyer 800**	**Piaggio P180 Avanti**	**Celera 500l**
Seats	11	10	10	7
Total Length (m)	17.4	-	14.4	11
Total Span (m)	19.2	-	14	16.7
Total Height (m)	3.84	-	3.98	-
Wing Span (m)	19.2	21	14	-
Wing Area (m2)	26	39.6	16	26
Winglet	Yes	Yes	No	Yes
Canard	No	No	Yes	No
Wing Position	Low wing	Low wing	Mid wing	Mid wing
Engine Pos, Number	Rear fuselage-side mounted (Puller),2	Wing (Puller),2	Wing (Pusher),2	Rear fuselage-backend (Pusher),1
MTOW (kg)	7484	-	5488	-
Cruise speed (km/h)	463	518	589	740
Service Ceiling (ft)	32000	35000	41000	30000
Range (km)	815	926	2800	8300

Regarding the method of calculations, the method used is strictly bound to what has been learned during lectures and considered to be the best methods because of those limitations. The calculations also use some tools such as USAF Stability & Control DATCOM, JavaFoil and supplementary programs like Microsoft Excel to acquire the numbers needed.

3. Results

 doi: 10.47355/AVIA.V5I2.94

e-ISSN: 2715-6958 p-ISSN: 2721-5342

3.1. Aircraft Conceptual Design

These are the latest designs of JMAF-18. These configurations are born in the results of past literature studies, preliminary calculations and through some iterations. The design will have a mid-wing configuration which has the best aerodynamic efficiency than other configurations because it uses less fairing which mean less interference drag. As the consequences of using mid-wing, the passengers cabin will be located in front of the wing and pushing the wing back to the aft-cabin. JMAF-18 also use another lifting surfaces such as canard to further boost the Cl and also as stability instruments. The configuration will have 2 engines mounted on the wing with a pusher type propeller to maintaining less noise to passengers cabin and providing the wing with undisturbed airflow. The tail used is a standard T-tail for getting an undisturbed airflow. The configuration is also be made with accessibility in mind creating a short aircraft with great stability. Some important parameters that aren't shown in here are also being considered and taken care of such as the propeller tip angle (>15 degrees), and cockpit design (maintaining space as regulated and the view angle).

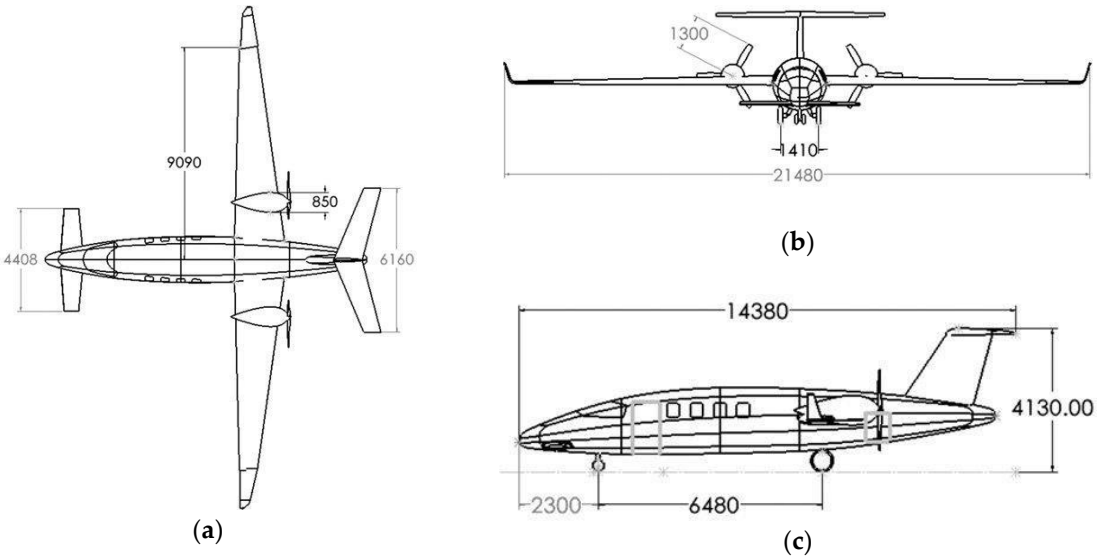

Figure 1. 3 view drawing of JMAF-18: (a) Top View (b) Front View (c) Side View

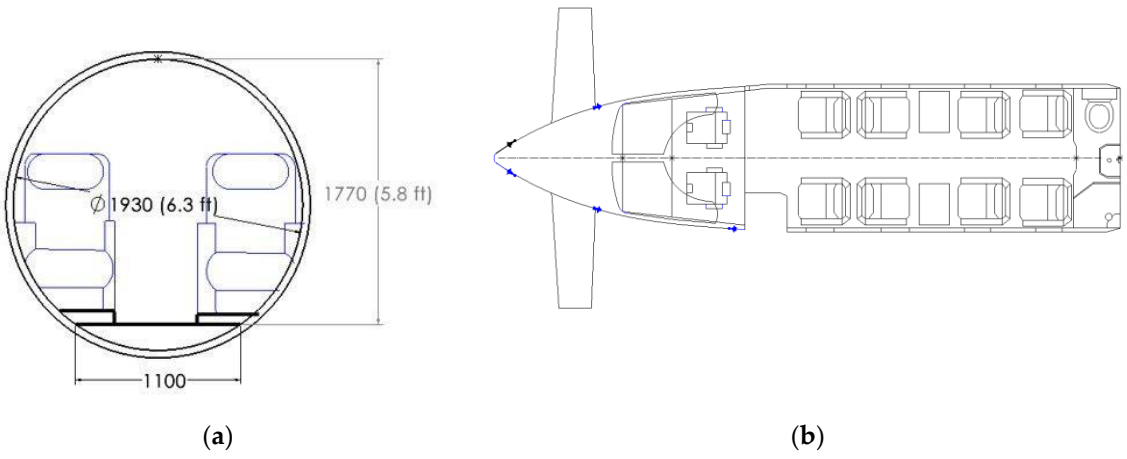

Figure 2. (a) Fuselage Cross-section (b) Fuselage Cabin View

Table 3. Geometry Data

e-ISSN: 2715-6958 p-ISSN: 2721-5342

	Wing	Canard	HTP	VTP
Aspect Ratio	12	5	5	1.2
Taper Ratio	0.34	0.6	0.6	0.6
Span (m)	18.18	4.4	6.16	2.1
Area (m^2)	27.55	3.88	7.59	3.68
MAC (m)	1.64	0.82	1	1.8
Swept (0.15c)	0	0	30	40
Incidence Angle (^{o})	3	3	0	0
Dihedral Angle (^{o})	0	0	0	0
Airfoil	NACA 6415	NACA 6415	NACA 0012	NACA 0012
Flap type	Fowler Flap	-	-	-

Table 4. Fuselage Geometry Data

	Fuselage
Total Length (m)	14.38
Cockpit Length (m)	1.6
Passengers Cabin Length (m)	5.18
Aft Cabin Length (m)	2.72

3.2. Design Point

The matching chart technique is used to determine the design point of the aircraft. The parameters used to create the matching chart is shown in Table 5. Additionally, the data from Piaggio Avanti and Eviation Alice are also used in order to narrow down the appropriate design point.

Table 5. Matching Chart Parameters

Design Point Parameter	Value
Wing Loading, W/S (N/m2)	2900
Power Loading (N/hp)	45
Takeoff Distance (m)	900
Landing Distance (m)	950
Rate of Climb at AEO (fpm)	1600

The resulting matching chart is shown in Figure 3 below. From the matching chart shown in Figure 3, it is apparent that the design points of Eviation Alice and Piaggio Avanti are located further on the right and below, which shows that both have higher wing loading and lower power loading than the design point. The JMAF-18 design point, however, cannot be in the same area as the other two as the design point is limited by the FAR 23 (parabolic curves) and the landing lift coefficients (vertical curves).

e-ISSN: 2715-6958 p-ISSN: 2721-5342

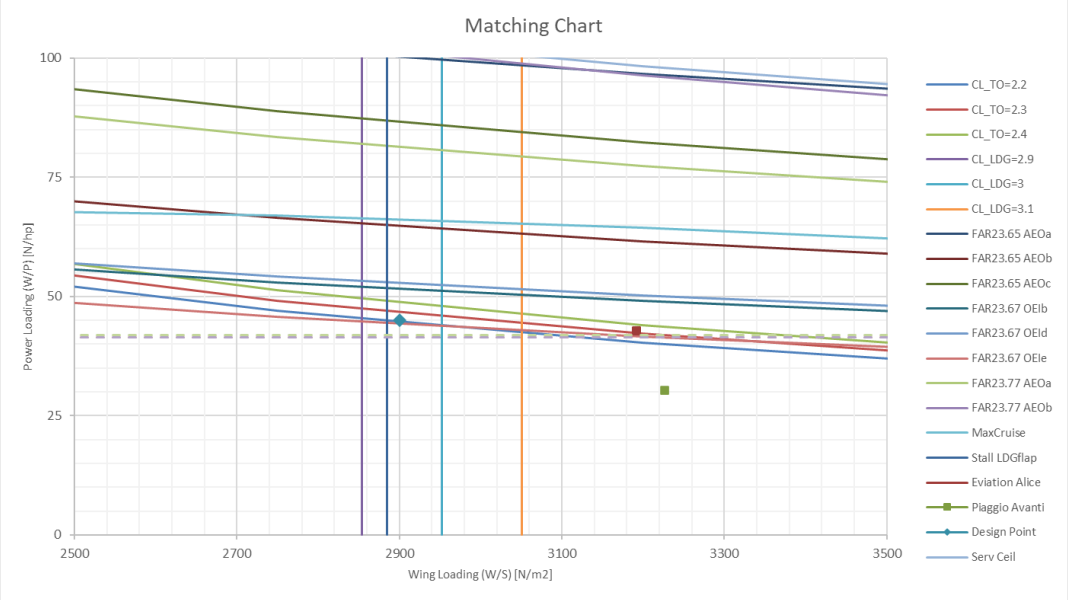

Figure 3. Matching Chart

3.3. Aerodynamic Analysis

The aerodynamic analysis is conducted by computing the aerodynamic coefficients of aircraft by utilizing the Digital DATCOM presented in Figure 4.

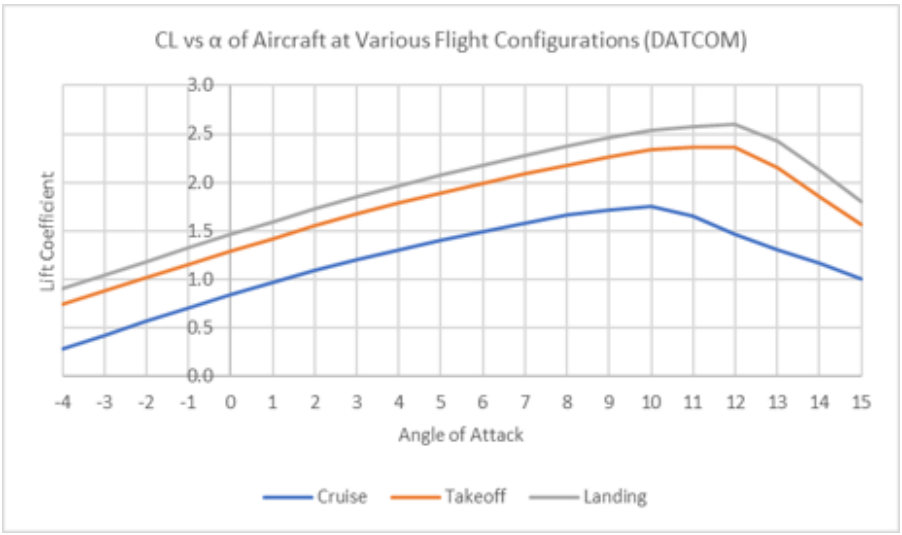

Figure 4. Lift Coefficient versus Angle of Attack

The required lift coefficient during cruise is 0.750. To generate enough lift in cruise condition, the aircraft will need to fly at angle of attack of around 0°. During the take-off, the required lift coefficient is 1.78 in which the flap is deflected 25°. This result in aircraft maximum lift coefficient of 2.367, thus the required lift during take-off is fulfilled at angle of attack of about 4°. In landing condition, the aircraft fulfilled the required lift coefficient of 1.10 at around 8° angle of attack. During landing, the flap is deflected 45°

e-ISSN: 2715-6958 p-ISSN: 2721-5342

Next, the drag polar is computed by calculating the component buildup from external aircraft parts that does not include the fuselage, empennage, and wing. This buildup is then added to the drag calculated by DATCOM. The results are shown in Figure 5.

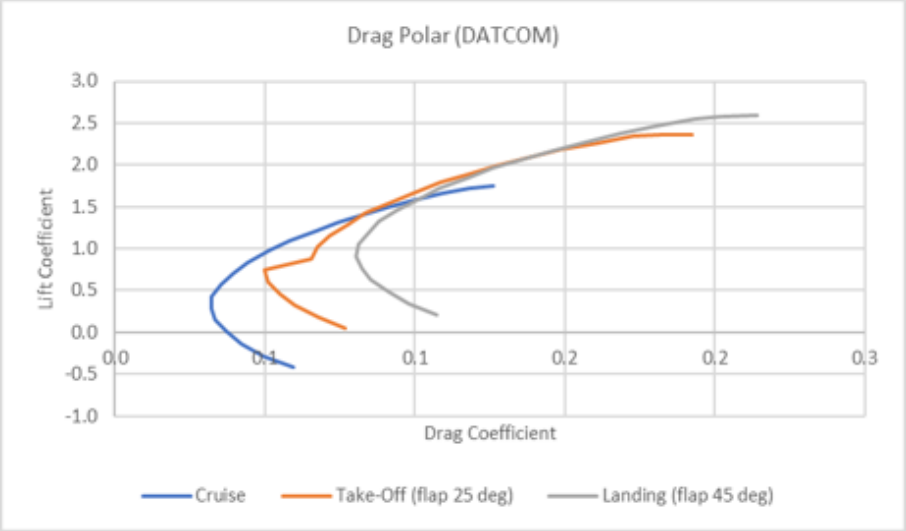

Figure 5. Drag Polar

Then, we want to know whether or not the aircraft is cruising at optimum L/D. This is done by computing the Lift-to-Drag ratio versus lift coefficient graph. As shown in Figure 6, it can be concluded that the L/D at cruise is 19.98 with CL of 0.84, which is already optimum.

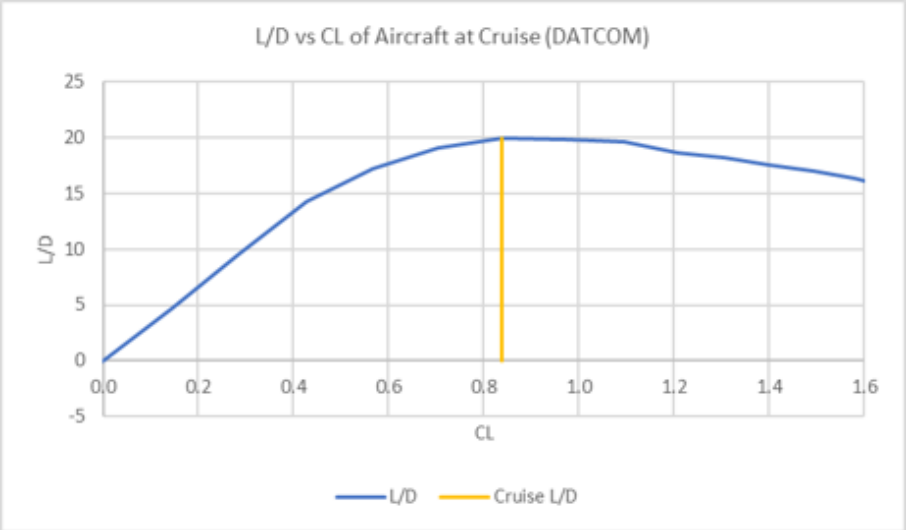

Figure 6. Lift to Drag Ratio versus Lift Coefficient

3.4. Weight and Balance

For the weight and balance section, the calculation of the weight of the components is using the method from reference [2]. This section is important because it will locate the centre of gravity of JMAF-18 aircraft. Based on the conceptual design; the breakdown of the weights can be seen in Table 6.

e-ISSN: 2715-6958 p-ISSN: 2721-5342

Table 6. Weight Breakdown

	Mass (kg)	Percentage Mass (%)
Airframe + Control	2670	37
Electric Engine	640	9
Operational Items	200	3
Total Batteries	2940	41
Passengers	800	11
Total	7250	100

Then for the calculation of centre of gravity, the calculation is using the moment forces (mass times distance to a reference point) of each component. Then by applying critical configurations of passengers that the aircraft will fly in; we can construct the potato diagram (centre of gravity shift diagram) that can be seen at Figure 7 below.

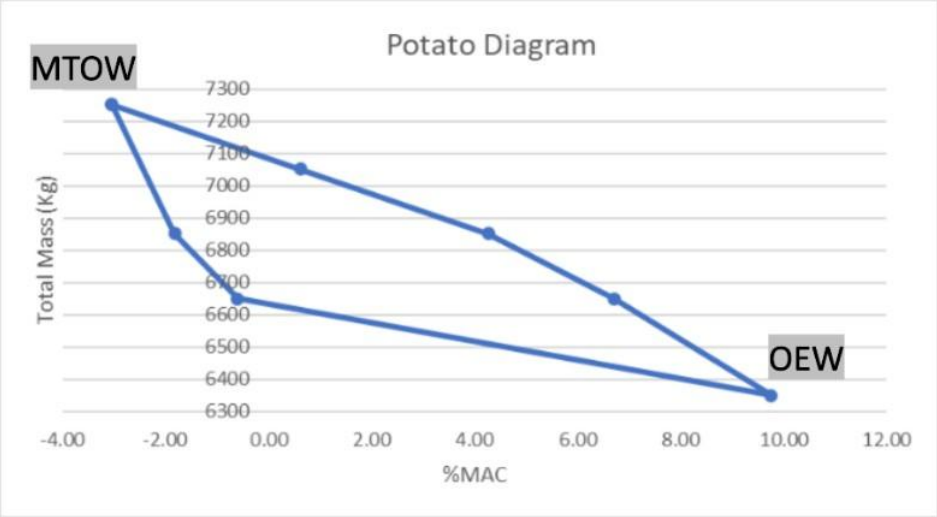

Figure 7. Potato Diagram

From the graph above we can locate the most forward and most aft centre of gravity; which is at -3% MAC and 9% MAC respectively.

3.5. Structural Layout

Modern day aircraft usually use alloys such as the Al-2XXX and Al-7XXX series or composites such as carbon fiber reinforced plastic (CFRP) and glass fiber reinforced plastic (GFRP). Through assessment of the aircraft design references [3] and [9], the aircraft will be using aluminum as it is relatively cheaper than composite and if combination is used between composite and aluminum, it is much more complex as they have different properties and cause a variety of structural problems. Assessed by weight and strength, the material usage would be as shown in Table 7.

The loads experienced by the wing – such as bending and shear – will be transported via the central wing box to the fuselage structure by our wing structure, which modifies the carry through structure. The spars will be the main structural component that carries most of the load from the wing and transfers it to the fuselage structure via the central wing box. The structure component of the empennage and canard are like that of the wing sections so to say they have ribs, spars and stringers. Although, the empennage carries a lower load when compared to the wing sections so the use of

e-ISSN: 2715-6958 p-ISSN: 2721-5342

stringers can be reduced. According to the reference [3], the ribs are spaced between 15-30 inches, and the front spar is 15-25% of chord length, while the rear spar is 70-75% of chord length. For the fuselage, the structural layout has components like bulkheads, frames and longerons. The placement and numbers of it is referenced from similar sized aircraft.

Table 7. Expected Material Selection

No.	Structure	Material
1	Frame	Aluminum series
2	Bulkhead	Aluminum series
3	Longeron	Aluminum series
4	Spar	Aluminum series
5	Rib	Aluminum series
6	Skin	Aluminum series
7	Stringer	Aluminum series

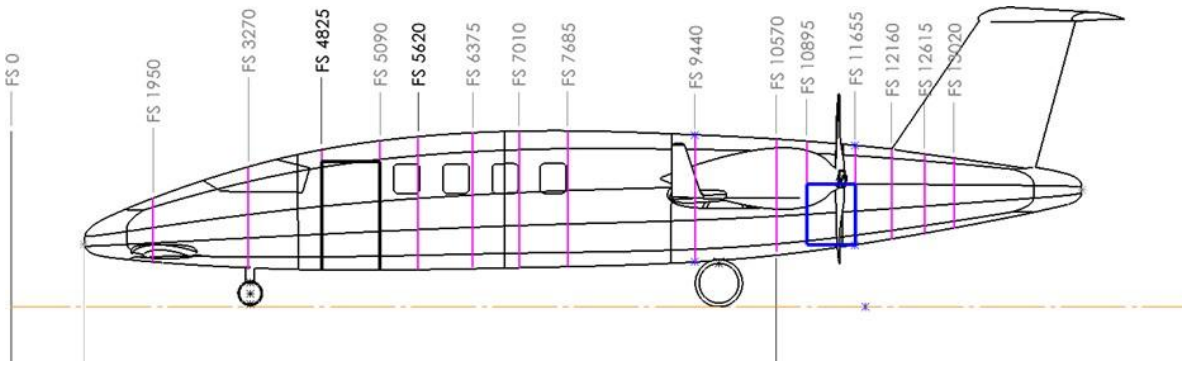

Figure 8. Fuselage structural layout

Table 8. Fuselage Structures

Structure	Placement	Numbers
Frame	FS 3270, FS 4285, FS 5090, FS 5620, FS 6375, FS 7010, FS 7685, FS 9440, FS 10570, FS 10895, FS 12160, FS 12615, FS 13020	13
Pressure Bulkhead	FS 1950, FS 11655	2
Longerons	-	14

The following table below summarizes the structural layout for the wing, empennage and canard.

Table 9. Structural Layout of the wing, empennage and canard.

Part	Wing	VTP	HTP	Canard
Main	15%c	20%c	15%c	15%c
Rear	70%c	65%c	65%c	65%c
Aileron	25%c			30%c
Rudder		30%c		
Elevator			30%c	
Flap	27%c			

 doi: 10.47355/AVIA.V5I2.94

e-ISSN: 2715-6958 p-ISSN: 2721-5342

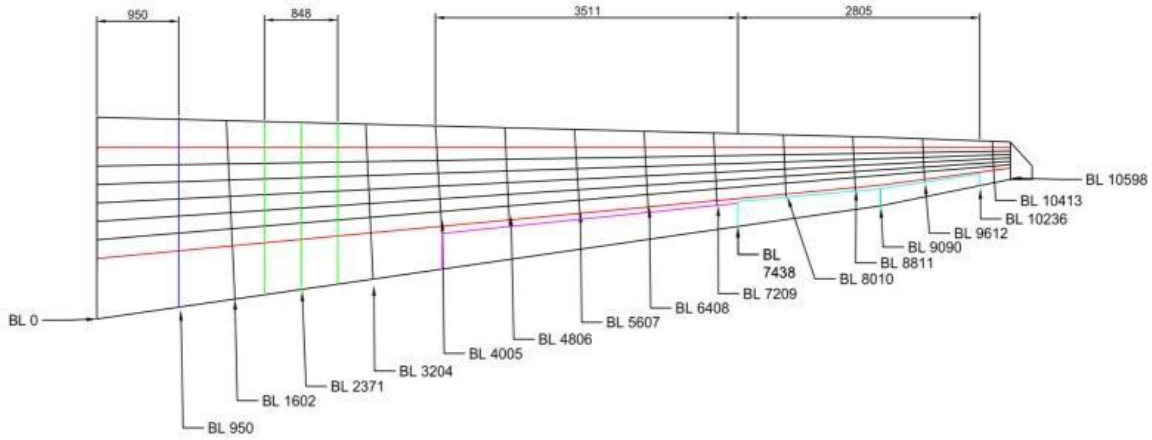

Figure 9. Example of the JMAF-18 structural layout with wing station number

3.6. Stability and Control Analysis

To achieve static stability, there are 3 most important parameters according to reference [13] there are Clß (-), Cmα(-), and Cnß(+). The Table 10 below shows the values of the parameters of the JMAF-18 aircraft for most forward and most aft configuration:

Table 10. Important Parameters of JMAF-18 Aircraft for Stability and Control Analysis

Parameters	Most fwd.(/rad)	Most aft (/rad)	Requirement	Typical Value (/rad)
Cmα	-3.05	-2.11	(-) Fulfilled	-0.7
Cnß	0.00024	0.00024	(+) Fulfilled	0.07
Clß	-0.07	-0.07	(-) Fulfilled	-0.07

As it can be seen from Table 10, the values of the aircraft correctly fulfil the important parameters for reaching static stability. Then when compared to the typical values; the Cmα value is three times larger than usual. This will result in a more stable aircraft but with the price of harder pitch control. The Cnß value is also significantly lower than usual, but that means it has easier control in lateral direction. The Clß value is very close to the usual value which means it is both stable and easier to control.

Then for the control capacity, it is necessary to check if the designed tailplane has fulfilled the requirements for stability and control. The function of control and stability boundaries are calculated according to reference [12] and is shown as a function of the HTP/Wing area vs the centre of gravity. The resulted calculations can be seen on the figure below:

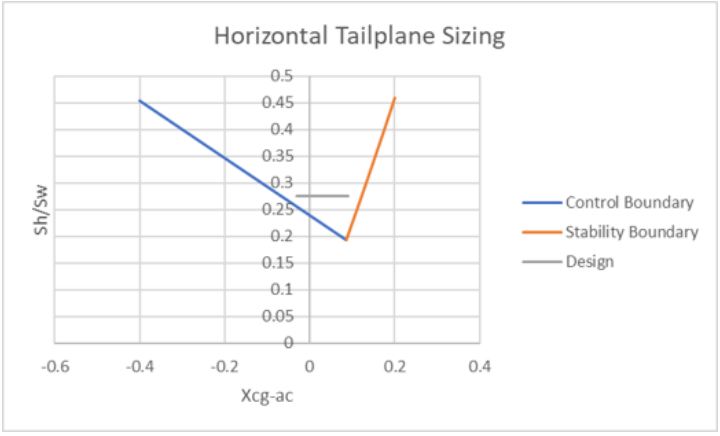

Figure 10. Horizontal Tailplane Sizing

e-ISSN: 2715-6958 p-ISSN: 2721-5342

It can be seen based on the figure above that the designed horizontal tailplane from Figure 10**.** Is both within control boundary and stability boundary.

3.7. Performance Analysis

To start the performance analysis of the aircraft, the drag polar at different flight configurations are recalled in order to determine the aircraft parameter. The drag polar is shown in the aerodynamic analysis of the aircraft.

Recalling the DRO, it is stated that the takeoff distance and landing distance of aircraft with MTOW and 0.95 MTOW shall not exceed 900 m and 950 m, respectively. Both takeoff and landing distances are determined using the algorithm for calculating airfield performance. The results are shown in the Table 11 and Table 12.

Table 11. Takeoff Distance

W (kg)	V_s (m/s)	V_{LOF} (m/s)	R (m)	γ_c (rad)	S_{ground} (m)	S_{trans} (m)	S_{TO} (m)
7250	43.3	51.93	1833	0.129	578	236	814

Table 12. Landing Distance

Distance	Value
Airborne distance (m)	306
Phase 1 ground distance (m)	500
Phase 2 ground distance (m)	46
Landing distance (m)	853

As JMAF-18 is not a single engine aircraft, balanced field length must be calculated as engine failure may occur during takeoff phase. The calculation is done by using the algorithm for calculating airfield performance also. Table 13 shows the results of balanced field length calculation.

Table 13. Balanced Field Length Calculation

Mass (kg)	Weight (N)	T_{OEI} (N)	$T_{OEI/W}$ (m)	V_{EF} (m)	STOD (m)	CTOD (m)	STOD-CTOD	BFL (m)
7250	71122.5	9757.4	0.137	52.1	2203	1551.9	651	1877

Table 13 shows that the balanced field length is 1877.498 m. This number is significantly large for takeoff distance of 814 m.

The DRO requires that the airplane have a minimum climb rate of at least 1600 fpm at sea level while carrying its maximum take-off weight for climb performance. The aircraft's climb rate was determined using the formula from [1], which calculates the rate of climb depending on excess power, where excess power is the power available (thrust x velocity) subtracted by the power required (efficiency x engine power) of a propeller aircraft.

Absolute ceiling is altitude where maximum rate of climb is zero where it is the highest altitude achievable in steady, level flight. Whereas service ceiling represents the practical upper limit for steady, level flight. So, to say, the graph of altitude versus rate of climb should be plotted where absolute ceiling occurs at (R/C)max = 0 m/s and service ceiling occurs at (R/C)max = 0.5 m/s. The endurance must be determined first, and then the range can be determined depending on the endurance. The battery capacity and the power required by the aircraft are used to calculate endurance. For the calculation below, the range and endurance of the flight to alternate was also included as mentioned already in our mission profile. In addition, the range of electric aircraft is

e-ISSN: 2715-6958 p-ISSN: 2721-5342

affected by the endurance and velocity, where the range-payload diagram is built upon this information and the payload is based upon the weight of the passengers and their luggage. Flight Envelope or also called as V-n diagram is a diagram that shows the range in which load factors can be applied to the aircraft at different velocity conditions of the aircraft and the Gust Envelope or also called the Gust V-n diagram is another diagram that displays the range that the aircraft is able to withstand load factors that are caused by gust in different velocities.

Figure 11 shows the rate of climb diagram and the payload-range that we have obtained.

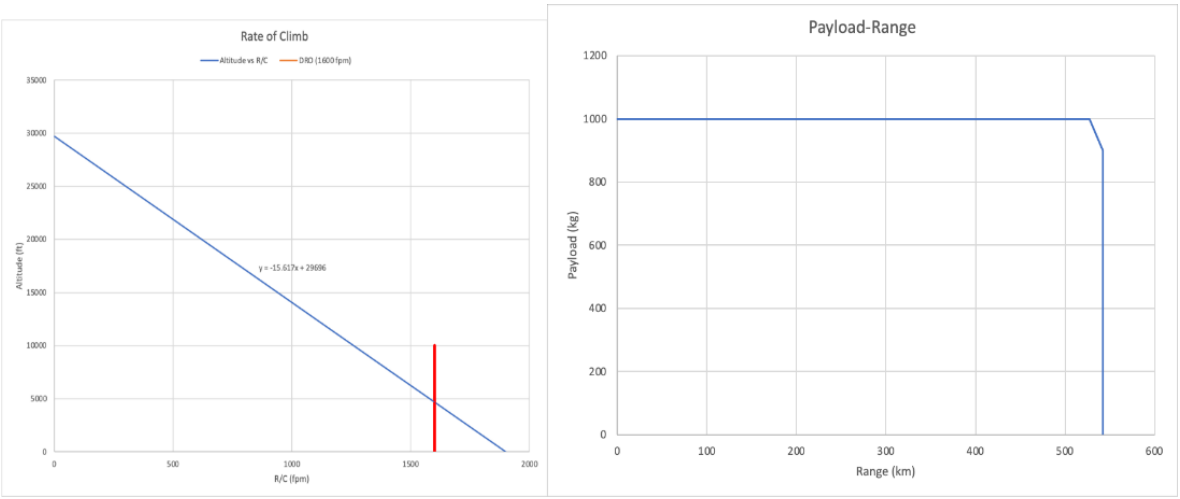

Figure 11. Rate of Climb Diagram (Left) and Payload-Range Diagram (Right)

Lastly, the flight envelope and gust diagram of the aircraft is also obtained as seen in Figure 12 below:

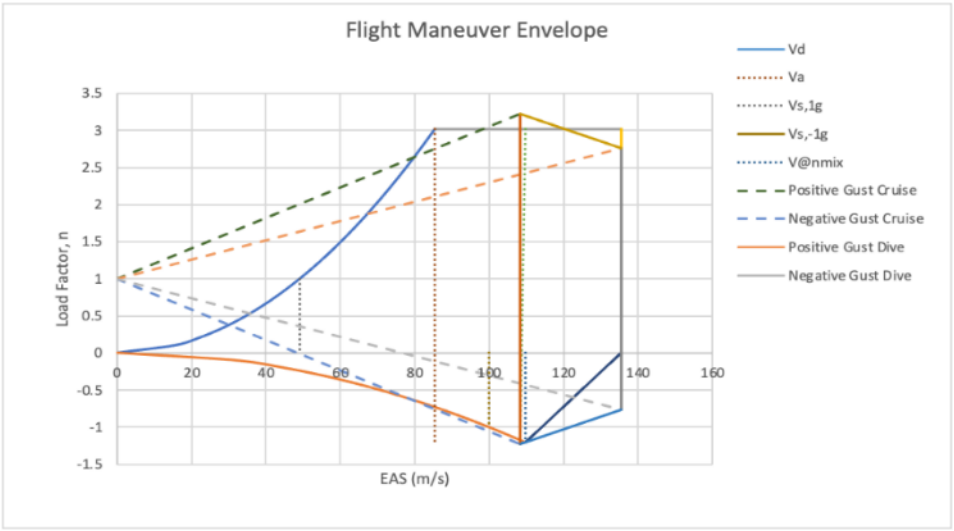

Figure 12. Flight Maneuver Envelope

3.8. Landing Gear Design

For the landing gear retraction, nose landing gear will retract to the front and main landing gear will retract to the aft cabin. The space needed has been calculated and will be discussed in Battery & Aft-cabin space management sub-section.

e-ISSN: 2715-6958 p-ISSN: 2721-5342

Table 14. Landing Gear Design

Landing Gear		
Nose Landing Gear location (m)		2.3
Nose Landing Gear diameter (m)		0.3
Main Landing Gear diameter (m)		0.525
Main Landing Gear location X from Nose (m)		8.78
Main Landing Gear location Y from mid fuselage (m)		0.7
Z ground from mid fuselage (m)		1.5
Tip back and Turn		
	Most fwd	Most aft
X cg (m)	8.05	8.26
Longitudinal tip over (°)	46.2	36.6
Nose Landing Gear Load	11.3 %	8.0 %
Main Landing Gear Load	88.7 %	92.0 %
Lateral tip over (°)	48.6	47.6

As stated on Table 14, the aircraft will have a longitudinal and lateral tip over of 46.2 and 48.6 degrees for most forward configuration also with 36.6 and 47.6 degrees for the most aft configuration which is stable (< 55 degrees). Also the nose landing gear load and main landing gear load are well within regulations.

3.9. Battery & Aft-cabin space management

The battery used will have these specifications according to ref [15]. The battery will be placed on both wing and aft-cabin. The wing will store 2.16 m^3 of battery while the rest of 1.81 m^3 will be stored on aft-cabin. Aft-cabin will hold the baggage, main landing gear, wing structure (front spar to rear spar), and batteries. The calculation of the space needed are an estimation considering the dimensions of each items.

Table 15. Battery Specifications

Battery		
Battery Power	300 Wh/kg	
Battery Weight/Cell	141 g	
Battery Dimensions	118 x 151 x 10.7 mm	
Battery Cells Needed	20851 cells	
Battery Placement	Wing	11340 cells
	Fuselage (aft-cabin)	9511 cells

The space available in aft-cabin will be approximated by using a truncated cone volume with the radius of 1.8 m and 1.25 m with 2.72 m in length. For the space taken, the space for the wing structure is approximated using a trapezoid volume and the space for the main landing gear is by using a simple box volume. It is necessary to know that this evaluation will yields a bloated volume for space taken, which will be a safe measure in order to make sure that the space is truly available.

e-ISSN: 2715-6958 p-ISSN: 2721-5342

Table 16. Aft-cabin space management

Aft-cabin		
Volume (m3)	Main landing gear	0.63
	Wing Structure	0.515
	Baggage	2
	Battery	1.81
Volume Total (m3)		4.96
Volume Available (m3)		5.022

3.10. Cost Analysis

Cost estimation analysis is done according to the methods from reference [3]. By considering the aircraft performance data, powerplant data, design and production factors, and cost factors, the RDTE cost and production cost is estimated. The powerplant data, however, did not use the assumption from method in reference [3], instead uses the estimate from reference [6]. The aimed output are the aircraft cost and production quantity in 2026. The results of cost analysis: breakeven point is at 225 units of aircraft, selling at approximately USD 3,500,000. After 225 units are sold in 2026, the JMAF-18 production shall generate profit.

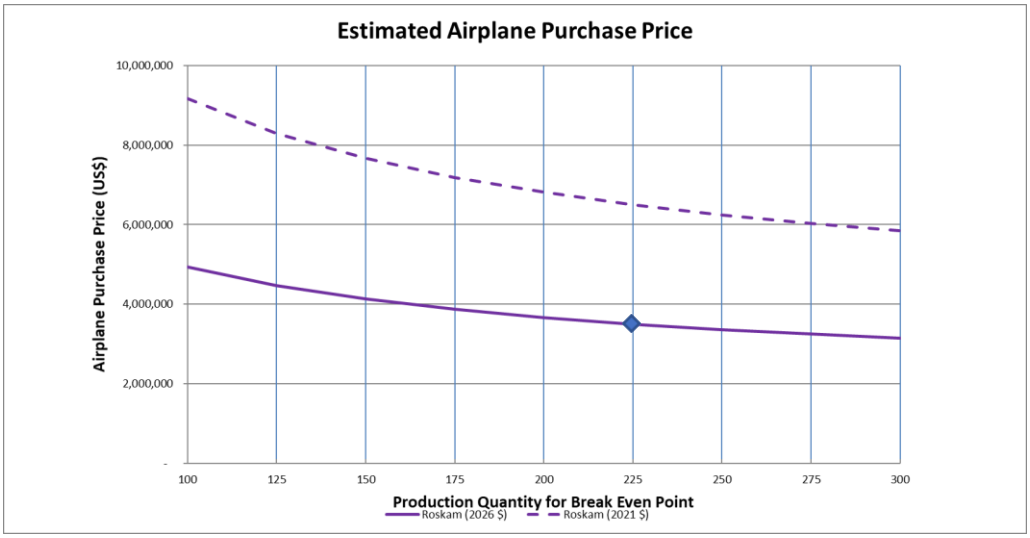

Figure 13. Cost Results

4. Discussion

To compare the resulted JMAF-18 aircraft to similar aircraft, in Table 17 below shows a throughout comparison between aircrafts that are already in production or still also at design phase. Throughout the process of this project, there were a lot of design changes that occurred due to various factors and from this we can learn that all our analysis that was analyzed and calculated interlinks strongly to its design. At this point, all the DRO points have been fulfilled so for now we may assume that the design is satisfactory.

e-ISSN: 2715-6958 p-ISSN: 2721-5342

Table 17. JMAF-18 Specification Comparison

	Eviation Alice	eFlyer 800	Piaggio P180 Avanti	Celera 500l	JMAF-18
Seats	11	10	10	7	10
Total Length (m)	17.4	-	14.4	11	14.38
Total Span (m)	19.2	-	14	16.7	21.48
Total Height (m)	3.84	-	3.98	-	4.13
Wing Span (m)	19.2	21	14	-	18.18
Wing Area (m^2)	26	39.6	16	26	27.55
Winglet	Yes	Yes	No	Yes	Yes
Canard	No	No	Yes	No	Yes
Wing Position	Low wing	Low wing	Mid wing	Mid wing	Mid wing
Engine Pos, Number	Rear fuselage-side mounted (Puller), 2	Wing (Puller), 2	Wing (Pusher), 2	Rear fuselage-backend (Pusher), 1	Wing (Pusher), 2
MTOW (kg)	7484	-	5488	-	7250
Cruise speed (km/h)	463	518	589	740	330
Service Ceiling (ft)	32000	35000	41000	30000	29675
Range (km)	815	926	2800	8300	542

5. Conclusions

Finally, the Table 18 below shows the comparison of the aircraft with the DRO. The MTOW that was calculated was less than the DRO, where we obtained the MTOW as 7250 kg. The range we have obtained seen from the payload-range diagram is 542 km at maximum payload and 623 km with 4 passengers on board. Lastly, from the previous slide we can see that the rate of climb at sea level that has been attained is 1902 fpm which fulfils the required DRO. In addition, we have obtained a takeoff distance of 814 m and landing distance of 852 m, which fulfils the prescribed DRO. Therefore, we can conclude that with the current results and analysis the aircraft has satisfy the conditions and since electric aircrafts are still being developed, we have taken a step forward in the future for net zero emissions.

Table 18. Conclusions

	DRO	JMAF-18
MTOW	≤ 8000 kg	7250 kg
Range	≥ 450 km	542 km
Range (4pax)	≥ 550 km	623 km
Take-off distance	≤ 900 m	814 m
Landing distance	≤ 950 m	852 m
Rate of Climb	≥ 1600 fpm	1902 fpm
Price per unit (by 2026)	≤ USD 3,600,000	USD 3,501,046

 doi: 10.47355/AVIA.V5I2.94

e-ISSN: 2715-6958 p-ISSN: 2721-5342

Acknowledgments
First of all, we would like to express our gratitude towards our supervisor Dr. Taufiq Mulyanto, S.T. for his support and help with all of our work that has been put in this paper. We also would like to thank the teaching assistants and our colleagues for the support and feedback.

References

1. Gudmundsson, Snorri. "General Aviation Aircraft Design: Applied Methods and Procedures." General Aviation Aircraft Design, Butterworth-Heinemann, 2014, doi:10.1016/c2011-0-06824-2.
2. Raymer, Daniel P. Aircraft Design: A Conceptual Approach. American Institute of Aeronautics and Astronautics, Inc, 1992.
3. Roskam, Jan. Airplane Design, Parts 1-8. DAR corporation, 1989.
4. Vries, Peter de. "Web Forum - What's the Optimal Cruise Lift to Drag Ratio of the Piaggio Avanti?" Aviation Stack Exchange, 21 June 2021, https://aviation.stackexchange.com/questions/87882/whats-the-optimal-cruise-lift-todrag- ratio-of-the-piaggio-avanti.
5. Chin, Jeffrey C, et al. "Battery Evaluation Profiles for X-57 and Future Urban Electric Aircraft." 2020, https://openmdao.org/pubs/chin_battery_evaluation_2020.pdf. Accessed 2021.
6. Patel K. "Lithium-Sulfur Battery: Chemistry, Challenges, Cost, and Future". 2016, https://www.researchgate.net/publication/319221333_Lithium-Sulfur_Battery_Chemistry_Challenges_Cost_and_Future. Accessed 2021.
7. Products. (n.d.). Retrieved December 10, 2020, from http://www.magnix.aero/products
8. Avanti P180 II. Specifications and Descriptions, PIAGGIO AMERICA, Inc., West Palm Beach, Florida, 2005.
9. 268 (200kW | 500Nm) - EMRAX - EMRAX | Axial flux e-motors. (n.d.). Retrieved December 10, 2020, from https://emrax.com/e-motors/emrax-268/
10. Baker, Alan, et al. *Composite Materials for Aircraft Structures*. Second ed., AIAA Education Series, 2004.
11. Howe, Denis. 2004. *Aircraft Loading and Structural Layout*. London and Bury St Edmunds: Professional Engineering Publishing Limited.
12. Traub, Lance W. "Range and Endurance Estimates for Battery-Powered Aircraft." Journal of Aircraft, vol. 48, 2011.
13. Prof. Dr. Scholz. 2021 *"Aircraft Design: Empennage Sizing"*. Hamburg Open Online University. (http://hoou.profscholz.de/)
14. Jenie, Y.I., & Muhammad, H. 2021. AE3220 Flight Dynamics Lecture Module 6: A/C Static Stability Analysis. Bandung: Institut Teknologi Bandung.
15. Dörfler, Susanne & Walus, Sylwia & Locke, Jacob & Fotouhi, Abbas & Auger, Daniel & Shateri, Neda & Abendroth, Thomas & Härtel, Paul & Althues, Holger & Kaskel, Stefan. (2021). Recent Progress and Emerging Application Areas for Lithium-Sulfur Battery Technology. Energy Technology. 9. 10.1002/ente.202000694.